

Progress in the applications of plasma surface modifications and correlations with the chemical properties of the plasma phase

J. AMOUROUX, A. GICQUEL, S. CAVVADIAS, D. MORVAN, F. AREFI
Université Pierre et Marie Curie, E.N.S.C.P.
Laboratoire des réacteurs chimiques en phase plasma
11, rue Pierre et Marie Curie, 75231 Paris, cedex 05, FRANCE

Abstract - Surface treatment of materials by plasma techniques depends essentially on the chemical properties of the boundary layers: plasma gas and solid surface. The first part of the paper presents the evolution of a non equilibrium plasma boundary layer and the molecule excitation correlated with its reactivity. Its applications to nitriding of the transition metals and silicon by NH_3 low pressure plasma indicates the role of the vibrational excitation during the surface treatment. The second part analyzes the properties of radicals and molecules in terms of polarizability and Lewis acid base reactivity. Plasma polymerization and etching are essentially developed for polymer surface treatments. In fine heat transfer and plasma chemical reactivity in a high pressure plasma torch for surface treatment of metal and silicon permit the understanding of the surface treatment of liquid or solid at high temperatures for nitriding or refining.

INTRODUCTION

The recent developments of plasma surface treatment impose to identify the new degrees of freedom of a chemical species excited by an electrical discharge.

Firstly we can remember that the chemical properties depend exclusively on the nature of the molecular orbitals, and consequently are modified by the electronic excitation created by the plasma. Generally the chemical reactivity increases with the vibrational level, the electronic excitation on π orbitals, the polarizability and the ionization.

However, the chemical properties of the plasma gases are modified through the boundary layer surrounding the target. The secondary electron, the electrical field, the heat and mass transfer are parameters which cause large modifications of the chemical composition and consequently of the reactivity.

In fact the surface treatment is directly correlated to the characteristics of the boundary layer (physical, chemical and electrical properties), plasma discharge conditions and depend on the surface modifications obtained. Nevertheless the influence of the nature of the target is a key parameter for the chemical reactions during the surface treatment: thus the modifications of heat and mass transfer between the gas boundary layer and the solid boundary layer according to the nature of the target control its surface modification.

In order to study some aspects of these processes, our aim is to present the modifications of the vibrational level of the chemical species in the boundary layer during the surface treatment for nitriding, the role of radicals and their main properties for polymerization and grafting phenomena and at last the heat and mass transfer by hot plasma surface treatment.

I. FUNDAMENTAL PROPERTIES OF A PLASMA GAS

Generally we can distinguish the non-equilibrium plasma from the equilibrium one, but the main differences existing between these two systems, in terms of chemical properties, result from the differences between thermal excitation and vibroelectronic excitation.

For an ETL plasma gas, Saha equation can be used to correlate the concentration of the ionized species with the temperature of the system. But a large part of the reactivity depends on the nature of the neutral excited species. For a complex chemical system, thermodynamic calculations provide the concentration field of the chemical species and energy consumption is function of the pressure and of the temperature... For example in the next thermodynamic diagram we can measure the evolution of the reductive properties of the complex chemical system C, H, O (fig.1). However the chemical reactivity in a plasma reactor depends on the vibroelectronic levels and on their life time which are unknown. As for a non-ETL plasma gas, Von Engel equation and Boltzman (1) equation (1) provide the possibility to calculate the electronic temperature as function of the size of the reactor. However the excitation of the different molecules, radicals and atoms depend on their cross

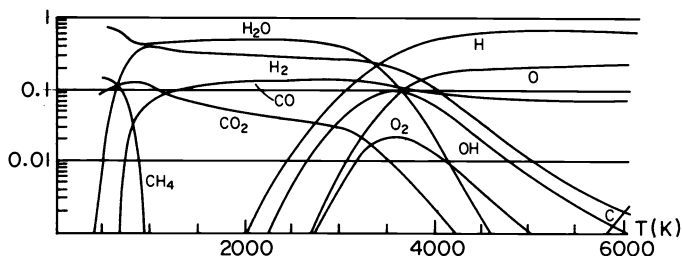


Fig. 1: Complex equilibrium chemical of C - H - O. Molar fraction versus T (K). O/C=4, C/H=1/9, P=1atm.

section as function of the energy of the electron and of the cluster molecule formation (2). In terms of the chemical properties, the energy transfer from the electron to the chemical species produces:

1. - new electronic states
formation of σ^* orbitals
triplet states
antibonding orbitals
2. - ion formation
negative ions (reduction properties)
positive ions (oxidation properties)
3. - modification of the molecular shape
modification of the symmetry, bond angle, hybridation
atom loss and radical formation
increase of the interatomic distance by vibrational excitation

That is to say that the chemical properties of the plasma mainly depend on the pressure and on the chemical composition (13).

However, the gas boundary layer produces large modifications of the chemical properties due to the heat and mass transfer between the gas and the target. Consequently, knowing only the plasma gas properties, does not provide those of the boundary layer. At last we have to take into account that our objective is a surface modification consequently our preoccupation concerns the chemical reactivity of the solid surface boundary layer which is quite different than that of the core of the target. The electronic excitation of the target by plasma gas impact, produced electronic diffusion, sputtering due to ion bombardement, diffusion of chemical excited species..., which explain its reactivity and the surface chemical modification. ESCA measurements allow to identify the fraction of the gas diffusing through the surface and who is responsible for the new chemical bonds.

II. MODIFICATIONS OF PLASMA REACTIVITY BY VIBRATIONAL EXCITATION

A large part of the plasma energy is stored on vibrational level of molecules and radicals. The chemical reactivity due to vibrational energy had been studied by Polanyi (4,5) for a non-equilibrium system, for instance in the following endothermic reaction $H + HF \rightarrow H_2 + F$. $\Delta H = 1.37$ eV (fig. 2) the evolution of the reaction rate depends on the energy distribution between the vibrational, rotational and the translational levels. So, for the same energy content in the chemical system, we can increase the reaction rate by a factor of 10^4 with a specific vibrational excitation. In the general case given below:



Polanyi presents an interpretation in function of the enthalpy of the reaction. In the next diagram (fig.3) we can notice that the exothermic systems are controlled by the energy barrier in the entrance valley i.e. by the translational energy of BC molecule, while the endothermic system are controlled by an energy barrier in the exit valley i.e. by the vibrational energy of the chemical specie BC.

These results point out that the reaction rate coefficient will be written as:

$$K = \int_0^\infty V_r (V, J, V' J', E_r) f(V_r T) dV_r$$

which takes into account of the different forms of energy controlling the transformation i.e. the vibrational and the rotational/translational energies of the molecules BC, and the relation kinetic energy E_r of the species.

II.1 DYNAMIC OF THE SURFACE REACTION MECHANISMS

Therefore the three main phases of a surface reaction are adsorption, chemical reaction, and recombination desorption. Nevertheless the surface phenomena can be controlled by a Langmuir-Hinselwood mechanism or a Rideal mechanism. In both of the cases the adsorption mechanism depends on the nature of the excited molecules and on the excited atoms of the lattice.

Wolken had calculated and demonstrated that surface reaction phenomena or recombination or desorption are characterized by an attractive exothermic step with the formation of desorbed vibrational excited molecules (6).

However the energy transfer between gas boundary layer and solid depends on the energy

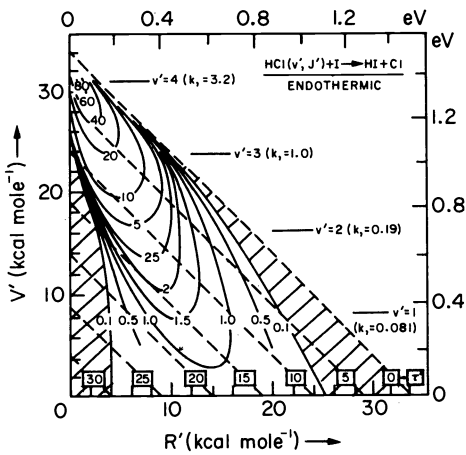


Fig. 2: Role of vibrational energy on the rate constant for endothermic reactions (4,5).

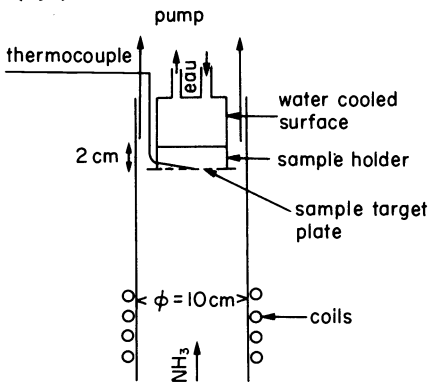


Fig. 4: Reactor scheme.

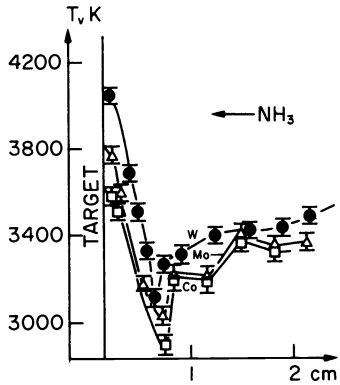


Fig. 6: Vibrational temperature according to the nature of the transitional metal.

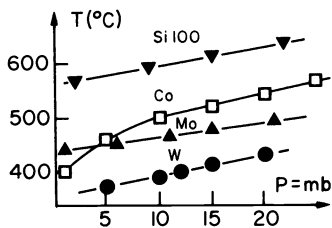


Fig. 8: Solid temperature versus pressure according to the nature of the metals.

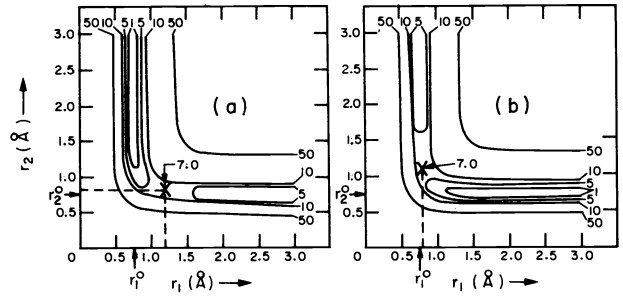


Fig. 3: Position of the activation barrier according to the exothermic (a) or endothermic (b) character of the reaction (4,5).

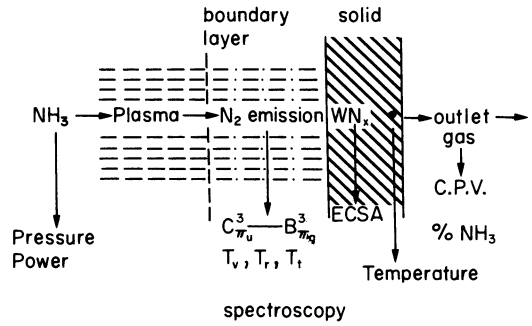


Fig. 5: Techniques of characterisation of the plasma and of the treated solid surfaces.

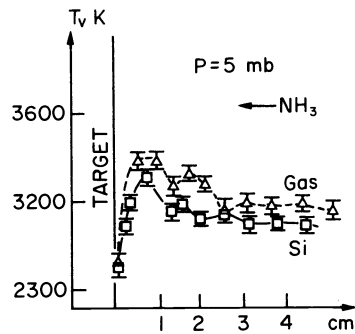


Fig. 7: Vibrational temperature in presence of silicon.

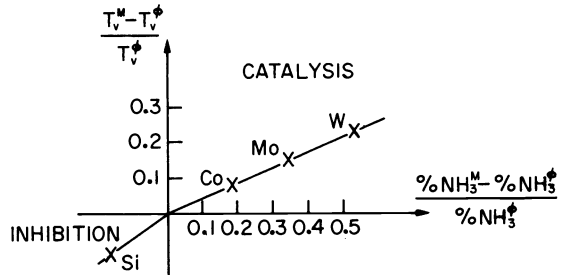


Fig. 9: Role of the vibrational temperature on the NH_3 decomposition rate.

transfer during the desorption process. Halpen and Rosner (7) propose an energetic partition (gas/target) such as $\beta = Q/\Delta n(D/2)$ for the nitrogen atom sorbed on transition metal surface. Generally for a nitrogen surface treatment where chemical reactions occur, β increases with the temperature, by contrast decreases with the temperature in the absence of surface reactivity.

II.2 EXPERIMENTAL STUDY OF THE BOUNDARY LAYER IN A NON-EQUILIBRIUM PLASMA OF NH₃ DURING ITS INTERACTION WITH A TRANSITION METAL TARGET (9,10,11)

The experimental studies of the boundary layers NH₃ plasma-metal target have been realized with an inductive RF plasma reactor (40 MHz) at low pressure (5-20 torrs) controlled by a direct emission spectrometer (UV-visible). The metal surface target is analysed by ESCA technique and Vickers microhardness (fig.4,5).

II.2.1 EXCITATION LEVEL OF N₂ MOLECULE IN A NH₃ PLASMA

The spectroscopic measurements of $C3\pi u \rightarrow B3\pi g$ transition gives us (12) a part of the vibrational modification of the system inside the boundary layer. The transition metal such as W, Mo, Co produce an increase of the vibrational excitation (fig.6,7) from 3400 K to 4200 K while the Si (100) target produces a decrease of the vibrational excitation from 3400 K to 2900 K.

II.2.2. HEAT TRANSFER ON THE TARGET (fig.8)

The measurement of the temperature of the target by a thermocouple indicates a large energy transfer for a silicon target against a smaller one for the transition metal target.

II.2.3. REACTION RATE OF NH₃ DECOMPOSITION (fig.9)

NH₃ decomposition is controlled by endothermic reaction ($2NH_3 \rightleftharpoons N_2 + 3H_2 \Delta H = 1 \text{ eV}$). By a gas chromatography analysis of the outlet gas, the data point out an increase of the reaction rate of NH₃ decomposition with an increase of the non-equilibrium state. These results are in agreement with the provisions of Polanyi and Wolken (4,6) for a system controlled by an endothermic reaction.

II.2.4. SURFACE MODIFICATIONS: ESCA ANALYSIS AND MICROHARDNESS

The surface nitriding analysis of the target is in agreement with the chemical reactivity of the plasma species in the boundary layer. the N/metal ratio increases (fig.10) with the vibrational level of the gas, and the microhardness measurements indicate the diffusion depth versus the treatment time (fig.11)

II.2.5. ROLE OF THE NH SPECIES

The NH emission spectroscopy is function of the chemical gas composition (N₂, H₂, or NH₃) indicates that one of the most reactive species responsible for the nitriding phenomena is NH radical characterized by its acid-base properties as function of its electronic excitation ($a'\Delta$, $b'\Sigma^+$, $C'\pi$) (3).

II.3. SURFACE NITRIDING PREDICTION

Nitriding phenomena of solid surface target consisting of transition metals are controlled by the nature of radical species such as NH and molecular species such as NH₃ and N₂ ($A3\Sigma u, B3\Pi g, C3\pi u$) (3,8). But the reactivity of the system depends on the vibrational excitation i.e. on the heat exchange between the excited gas boundary layer and the solid layer. The chemisorption mechanisms are the key step of the system, an increase of the excited level increases the nitriding while a quenching system (silicon) increases the heat transfer to the solid without chemisorption phenomena. These results suggest that the sticking probabilities of N₂, NH₃ or NH on W depend on the vibrational state. According to Wolken theory we can conclude that the energy barrier of the fundamental adsorption hypersurface corresponds to an attractive phenomena influenced by the vibrational level of the electronic states of the molecules. A modification of the gas pressure or of the chemical composition of the gas mixture controls the nature of the electronic states and the chemical properties of the system allowing a suitable surface treatment.

II.4. CASE OF A SILICON JUNCTION TYPE P(fig.12)

In order to determine the role of the impurities present in a lattice, we have compared the properties of a diode p treated by different plasma gas compositions (N₂, N₂ - H₂, NH₃, H₂). The ESCA analysis of the target indicates the presence of different chemical bonds (Si - B, B-O, B-H and B metal). The surface treatment in the same experimental conditions by the different plasma gas point out that the nitrogen or hydrogen reaction with the lattice

depend on the nature of the chemical bonds between Boron, Silicon, and oxygen impurities, for example nitrogen plasma transforms specifically Boron atom of the lattice in B-N compound while NH₃ plasma produces BN and B-Si-H compounds.

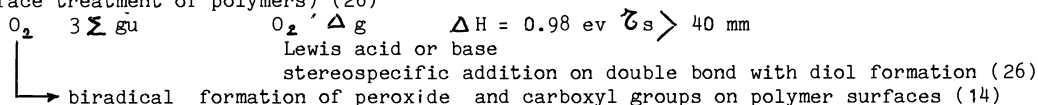
These results demonstrate the role of the chemical composition of the material during the surface treatment and the specific action of activated species such as N₂, NH, NH₃ or H₂ on the chemical bond of the lattice.

In conclusion of this part, the nitriding surface treatment requires a good understanding of the boundary layer of the plasma observed by emission spectroscopy and of the target surface chemical composition measured by ESCA or SIMS techniques.

III. CHEMICAL REACTIVITY OF RADICALS AND IONS - APPLICATIONS TO POLYMERIZATION, ETCHING PROCESSES, OR POLYMER SURFACE TREATMENT

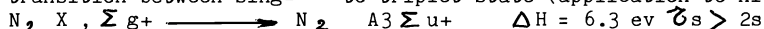
During the electronic excitation we observe the formation of odd electrons and vacancy orbitals, which modify the chemical properties of radicals, ions or molecules. For example we can present some classical excitation phenomena:

- transition between triplet state to a singlet state for O₂ molecule (application to surface treatment of polymers) (26)



biradical formation of peroxide and carboxyl groups on polymer surfaces (14)

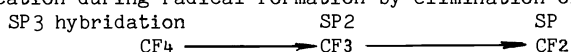
- transition between singlet to triplet state (application to nitriding of metal)



The odd electrons of the antibonding orbital are responsible for the high reactivity of N₂ chemisorption and nitride formation (nitriding of titanium)

- molecular shape and hybrid orbital (27) (application to etching or polymerization)

modification during radical formation by elimination of atoms



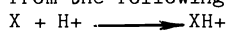
The loss atom of CF₄ molecule induces a modification of the bond angle and an increase of the reactivity from the odd electron and lone pair of electrons (Lewis base)

- polarizability (fig.13)

In the boundary layer the increase of the polarizability of the molecule, or radical is related to the electric field strength, consequently the viscosity of the gas phase is modified and the dipole-dipole interaction modified the surface properties during the treatment of polymer or induced a specific polymerization (C₂ H₂ F₂ gas gives piezoelectric polymer) while the acrylonitrile molecule is mainly grafted on the cathode by corona polymerization surface (15).

III.1 ACID-BASE PROPERTIES OF THE PLASMA SPECIES (16)

These mechanisms can be correlated with the Lewis acid base properties of the molecule or radical. Walter and Franklin (3) have determined the proton affinity for a large number of molecules from the following reactions:



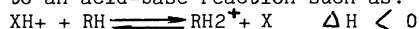
Lewis base

$$\Delta G \neq \Delta H \quad \Delta H = -(\text{PA})\text{X} \text{ or proton affinity of examples for a}$$

number of species (18)

| atoms | KJ/mole | molecules | KJ/mole (fig.14) |
|-------|-----------|------------------|------------------|
| O- | PA = 1600 | NH ₂ | PA = 1670 |
| F- | PA = 1550 | CF ₃ | PA = 1570 |
| Cl- | PA = 1400 | PH ₂ | PA = 1525 |
| F | PA = 330 | NH ₃ | PA = 880 |
| Ar | PA = 330 | H ₂ O | PA = 700 |
| | | HF | PA = 550 |

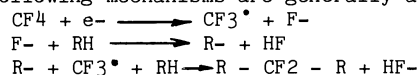
An association of these chemical species in the boundary layer or on the surface of the material leads to an acid-base reaction such as:



$$\Delta H = (\text{PA})\text{X} - (\text{PA})\text{RH} < 0 \text{ for a spontaneous reaction.}$$

These results show that the energy exchange in the acid-base reaction are one or two orders of magnitude higher in the gas phase than in the liquid phase (19,20,21).

Such phenomena occur in the grafting of fluorocarbons on polymer surfaces for which the following mechanisms are generally admitted:



These mechanisms which occur in a plasma surface treatment are complex due to the reaction of the first polymer layer with the core of the material. Diffusion, charge transfer and crosslinking take place during these mechanisms.

| | Standard samples | | | treated W samples P=5 mbar, P I=1kW, F-r=0.3 l/min, t=1.5 h | | | |
|---|------------------|----------|------------------|--|---|---|----------------|
| | W | WN | W ₂ N | NH ₃ | N ₂ -H ₂ 80%-20% | N ₂ -H ₂ 50%-50% | N ₂ |
| W _{405/2} | 242.6 eV | 244.5 eV | 247.5 eV | 244.3 eV 247.8 eV | 247.8 eV | 247.3 eV | 246.7 eV |
| N _{1s} | — | 397 eV | 397 eV | 396.7 eV | 396.2 eV | 396.5 eV | 396.6 eV |
| % W | 100 % | — | — | — | — | — | 10 % |
| % WN | — | 100 % | — | 80 % | — | — | — |
| % W ₂ N | — | — | 100 % | 20 % | 100 % | 100 % | 90 % |
| N _{1s} /W _{405/2} (N fixation rate) | | | | 2.3 | 1.0 | 0.8 | 0.3 |

Fig. 10: ESCA results. Identification of the new bonds created on tungsten by various plasmas.

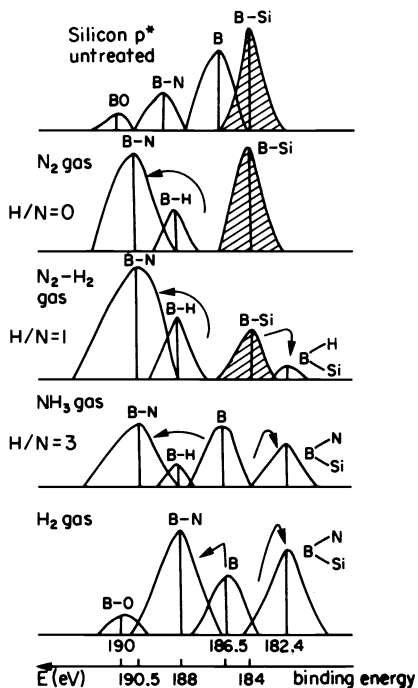


Fig. 12: Modification of the silicon surface according to the nature of the plasma.

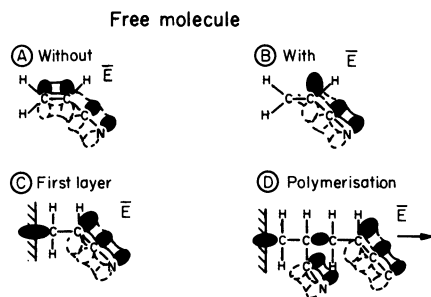


Fig. 13: Mechanisms of acrylonitrile molecule grafting on a cathode surface (15).

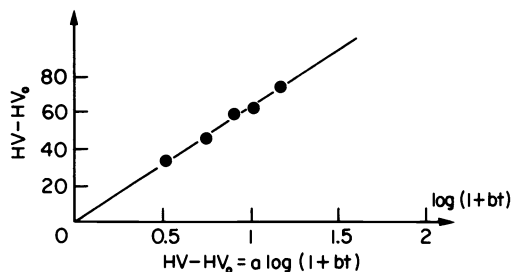


Fig. 11: Law of microhardness variation into the metal after treatment.

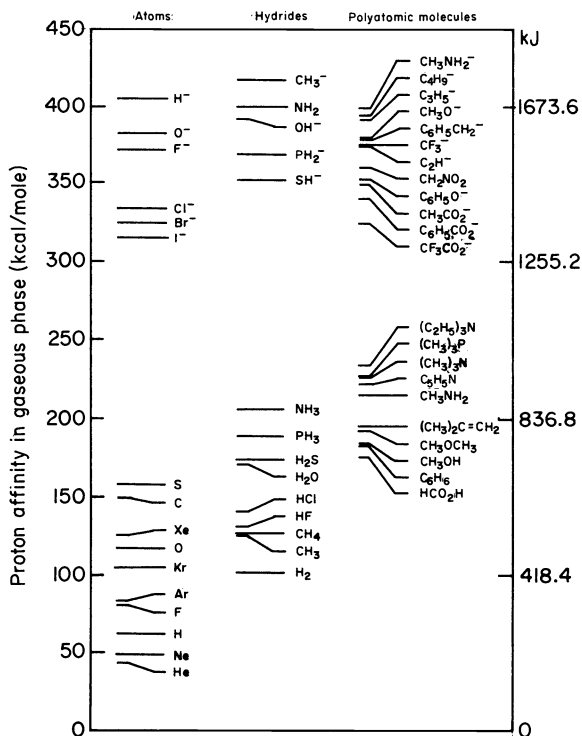
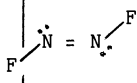
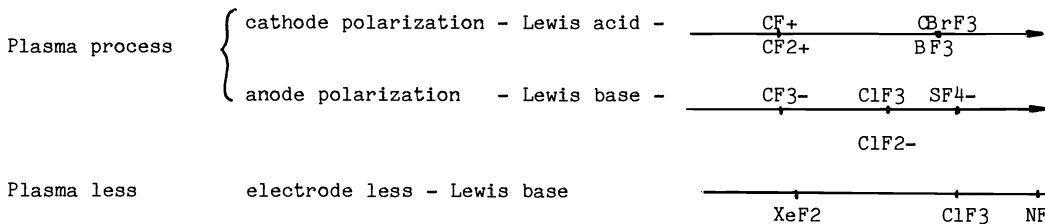


Fig. 14: Proton affinity scale in the gas phase. (From R. McIver; Science (1981) 39, 103.)

Fig. 15 Radicals - shapes and properties

| | | | | |
|--------------------------|---|--|--------------------------------------|--|
| Tetraedrique shape | | Planar molecule | | Planar molecule |
| Bond angle 109° | | bond angle 120° | | Bond angle 120°/180° |
| Hybridation SP3 | | hybridation SP2 | | hybridation SP2/SP |
| molecule | negative ions or molecule Lewis base | positive ions Lewis acid | radical | biradical or Lewis acid |
| CH4 109° | CH3- | CH3+ | .CH3 | :CH2 (carbene) fond state singlet excited state singlet 1Σ triplet 3 |
| CF4 109° | CF3- | CF3+ | .CF3 | :CF2 singlet state 105° Lewis acid triplet state 150° biradical time life 1 s at P205 |
| CCl4 | CCl3- | CCl3+ | .CCl3 | .CCl2 |
| CHF3 | | | | :CF2 + HF :CF2+ + HF- |
| CHCl3 | | | | :CCl2 + HCl |
| CBrF3 | CF3- | CF3+ | .CF3 | :CF2 |
| SiF4 weak Lewis acid | SiF3- | SiF3+ | .SiF3 | :SiF2 lifetime 150 s |
| SiH4 | SiH3- | SiH3+ | .SiH3 | :SiH2 |
| NF3 102° | NF2-  | | .NF2 | ·NF |
| NH3 | NH2- strong Lewis base (110°) | | odd electron in π orbital Lewis base | :NH biradical π fond state triplet state XΣ ⁺ excited state singlet state Δ, Σ ⁺ Lewis acid |
| ClF3 |  etching rate 5000Å/mn | | .ClF2 (F--F--F) SP Lewis base | BF3 120° Lewis acid |
| BrF3 | Lewis base etching rate 50.000 Å/mn | | | |
| <u>complex molecules</u> | | | | |
| XeF2 |  F--F 180° Lewis base etching rate 45 000Å/mn | | | |
| IF5 |  Lewis base | | | |
| SF6 |  Lewis base | | | |
| | | SF4 101°  Lewis base | | |
| | | SOF2 87°  Lewis base | | |

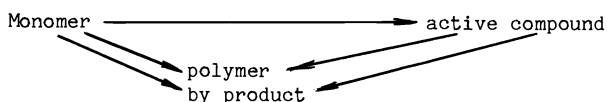
In order to point out the correlations between the chemical properties and the molecular structure we have collected in the above table some classical species employed for the etching and polymerization processes (fig.15). The etching processes therefore followed three main ways:



These results are in agreement with the ESCA analysis of the silicon boundary layer which point out in the case of a cathodic polarization the presence of CF+ CF2+ CF3+ in the lattice of silicon for 100 or 200 Å of depth (22). In the anodic polarization has given rise to F⁻ and SiF bonds (fig.16,17).

III.2 POLYMERIZATION PROCESS (25)

Large applications of plasma polymerization are controlled by different activation mechanisms such as ionic mechanisms, radical or photonic activation. However in a plasma reactor the three phenomena generally occur and produce polymers which are more complex and highly crosslinked. Nevertheless we have to consider the degradation phenomenon due to plasma polymer interactions, as it has been summarized by Yasuda in the following scheme (23).



The kinetic simulation (24) of these mechanisms explains the deposition growth of the polymer film, the ashing or the etching rate.

However the polymerization phenomena depend on the nature of the substrate and we can consider the different interactions between radicals or ions with the substrate.

1. - interaction between substrate and radicals
 - non-volatile species formation: grafting on polymeric materials
 - volatile species formation: etching or ashing
2. - no interaction between the substrate and radicals
 - deposition phenomena
3. - interaction between the lattice of the substrate and radicals
 - diffusion, or doping

As for the fluorocarbons we have studied the polymerization phenomena of C₂ H₂ F₂ on different materials such as silicon, glass, and the polymer films of PET and PP with a glow discharge and a corona discharge.

The glow discharge polymerization on silicon gives rise to a film layer with a thickness which depends on the plasma power and pressure, ESCA analysis of the material shows the main radical and chemical bonds existing at the surface such as CF₂, CF., C₂F which are in agreement with the thermodynamic calculations (fig.18, fig. 19).

For a PET film treated by corona discharge in an atmosphere of C₂ H₂ F₂ we observe (fig.20) the formation of polymer film and fluor grafting on the polymeric surface (28),(29).

At last on glass substrates, a treatment with CF₄ fluorocarbon gives rise to the diffusion of fluor atom in the lattice through a depth of 0.2 to 0.3 μm (fig. 21, fig. 22).

These results clearly demonstrate the role of the material during the surface treatment; finally we have pointed out the competition between radical formation on the surface by using a mixture of C₂ H₂ F₂ and air (fig.23,24,25). In the presence of oxygen, the fluorocarbon radicals are partly destroyed by oxidation (fig.25), and therefore give rise to short chains of oligomer which are soluble in solvents such as water and acetone and consequently did not meet the purposes of the surface treatment (36,37,38,39).

In other words oxygen present reacted immediately with the carbon radicals formed at the surface of the polymeric film and in this way avoided the grafting of the fluorocarbon groups onto the surface of the polymer. These results have been obtained by ESR analysis and dielectric measurements (31).

At last an incorporation of metals such as Na, K, Mg, Al, Sn, Cu... by using organometallic species, metal fluoride or chloride, or by sputtering permits to prepare semiconducting polymers (30,32,33,34,35).

IV.HIGH TEMPERATURE PLASMA SURFACE TREATMENT

COMPARISON OF EFFICIENCY OF THERMAL PROPERTIES AND CHEMICAL PROPERTIES

Thermal processes combined with chemical effects are responsible for surface treatment by high temperature plasma gas. In this case we have to take into account the evaporation phenomena of surface layer, melting phenomena and convective movement in the molten phase. However synthesis between evaporated material and plasma phase lead to new products in the boundary layer, these processes allow complex surface treatment by condensation or deposition phenomena.

IV.1. THERMODYNAMIC PROPERTIES OF A THERMAL PLASMA

At high pressure, higher than 200 torrs, plasma equilibrium processes are described by Saha's equation which allows to obtain the concentration in ionized species i.e. the oxidation property of the plasma gas (fig.26).

By using thermodynamic calculations (40,41,42) with the partition function of each species (ion, atom, radical, molecule) present in the chemical system, and by solving the Boltzmann equation by the method of Chapman and Enskog, we are allowed to determine transport properties for a single gas or a mixture. For example, the thermal conductivity of an Argon - H₂ mixture depends essentially on the hydrogen concentration and point out the rapid modification by the substitution of H₂ by N₂ (fig.27).

In agreement with these calculations, the complex boundary layer properties are probably far away from the main gas chemical and physical ones.

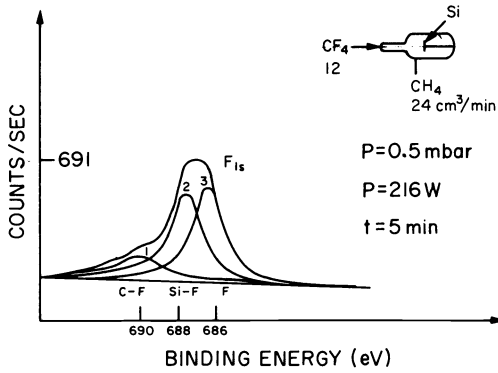


Fig. 16: Decomposed F_{1s} peak (ESCA analysis) for the pretreated silicon.

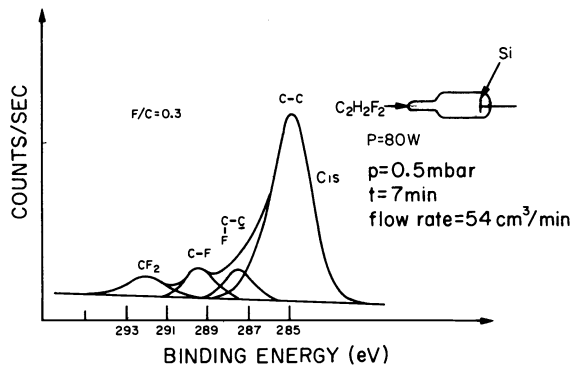


Fig. 19: Decomposed carbon peak of ESCA analysis for the pretreated silicon in an atmosphere of $C_2H_2F_2$.

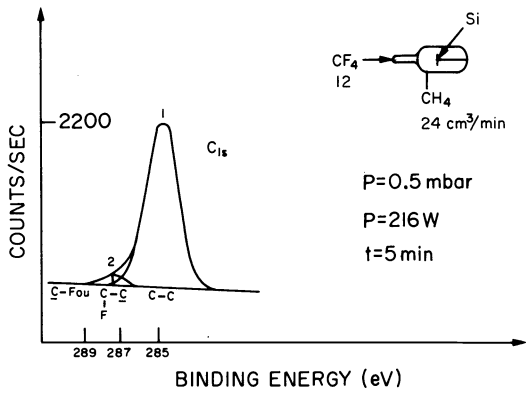
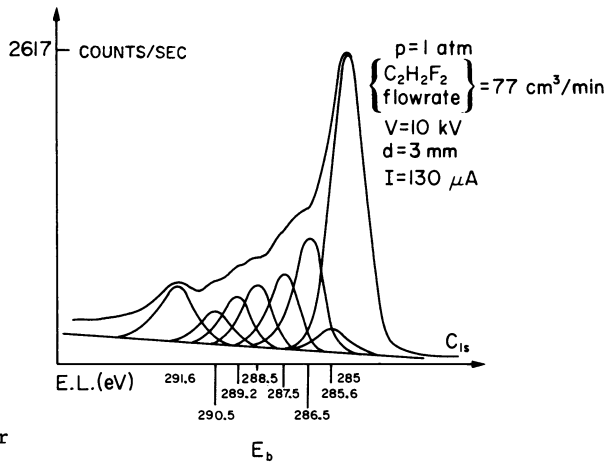


Fig. 17: ESCA analysis of the carbon peak for the pretreated silicon.



| E_b | Assignment |
|-----------------|-------------------------------|
| 285 | CH_2-CH_2 |
| 285.6 ± 0.1 | $CH_2=CF_2$ |
| 286.5 ± 0.1 | $-CH_2-CF_2-$, C-O |
| 287.4 ± 0.2 | $>C=$ C-F bonding in position |
| 288.6 ± 0.2 | $-CFH-CFH-$, $>C=O$ |
| 289.3 ± 0.2 | $-CFH-CF_2-$, $C=O-H$ |
| 290.2 ± 0.2 | $-CF_2-CH_2-$ O |
| 291.6 | $-CF_2-CFH$ |

Fig. 20: Decomposed carbon peak of ESCA analysis for the pretreated PET film.

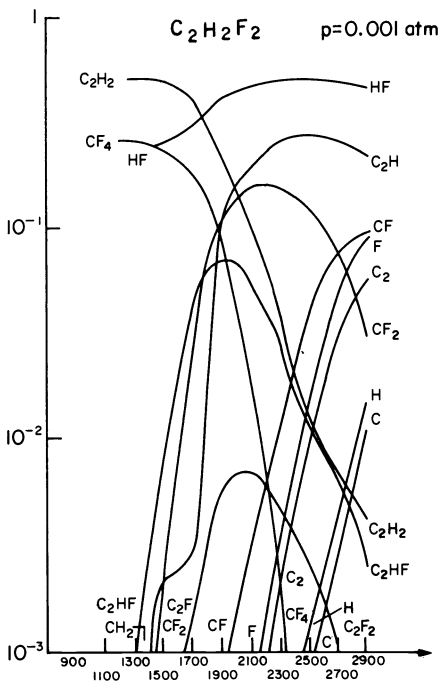


Fig. 18: Complex chemical equilibrium diagram for the stoichiometry $C_2H_2F_2$.

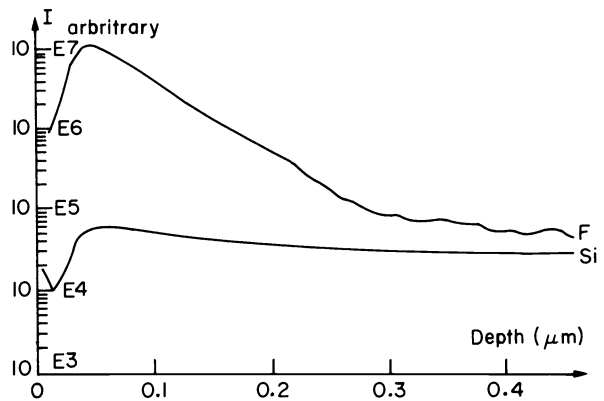


Fig. 21: SIMS depth profiles of silicon and fluorine. Discharge conditions: $T=200^\circ C$, $V=8kV$, $d=0.5$ mm, CF_4 flowrate: 0.45 l/h.

| | E_b (eV) | X/Si _{2p} |
|----------------------|------------|--------------------|
| C _{1s} | 285 | 6.2 |
| | 288.8 | |
| | 291 | |
| O _{1s} | 532.5 | 2.3 |
| F _{1s} | 685.2 | 2.4 |
| Na _{1s} | 1072.5 | 0.65 |
| Ca _{2p} 3/2 | 347.6 | 0.7 |
| Si _{2p} | 103.2 | 1 |

Fig. 22: ESCA ratios. Discharge conditions: T=200°C, V=8 kV, d=0.5mm, CF₄ flow-rate: 0.45 l/h.

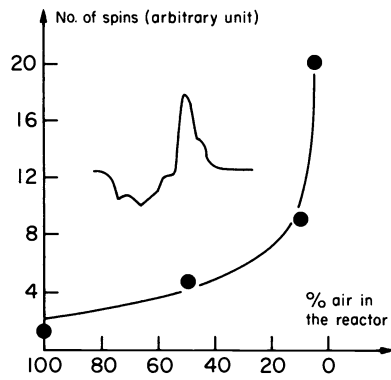


Fig. 23: Variation of free radical concentration as function of the residual air in the reactor. t=2.8 sec., Ar flow-rate=280 cm³/min, P=1 atm, PP thickness=18µm.

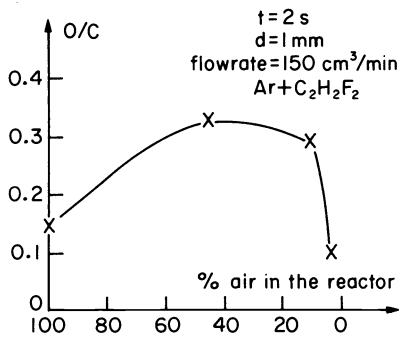


Fig. 24: O/C ratios obtained by ESCA analysis as function of the residual air in the reactor.

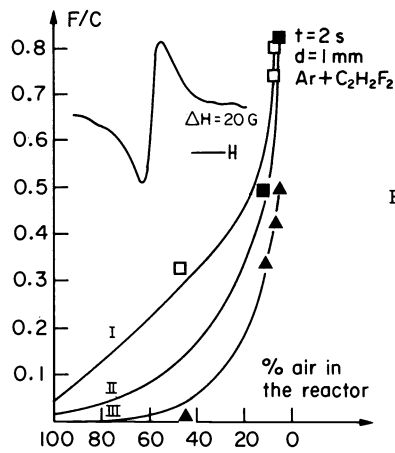


Fig. 25: F/C ratios obtained by ESCA analysis in function of the residual air in the reactor. PP pretreated I- after treatment II- washed 1h in H₂O III- washed 1h in H₂O and 1h in acetone.

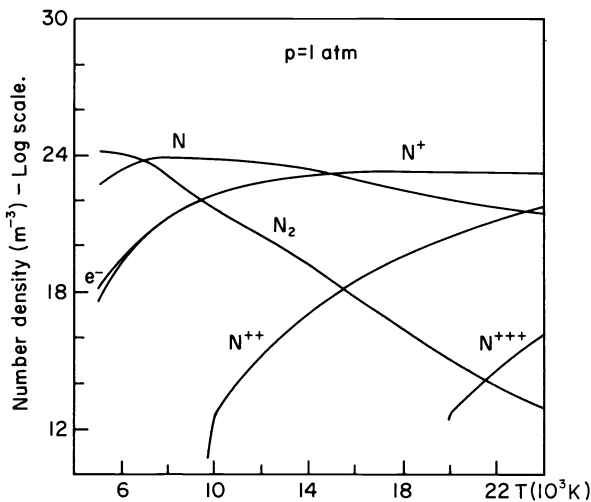


Fig. 26: Equilibrium composition of a nitrogen plasma (from ref (40)).

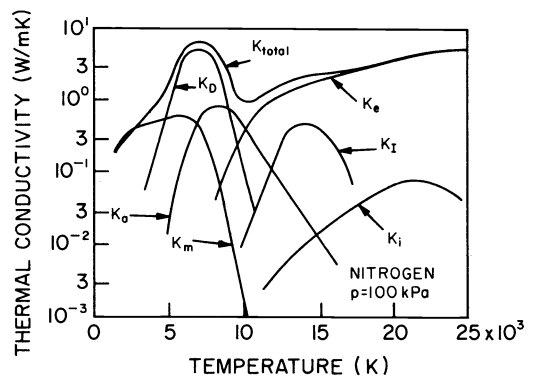


Fig. 27: Individual contribution to the thermal conductivity of a nitrogen plasma (61). Contribution due to:

- K_m : molecules
- K_a : atoms
- K_e : electrons
- K_i : ions
- K_D : dissociation
- K_I : ionisation
- p : 1 atm

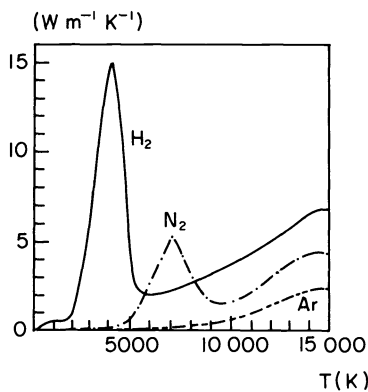


Fig. 27(a); Evolution of thermal conductivity of H₂, N₂ and Ar versus the temperature.

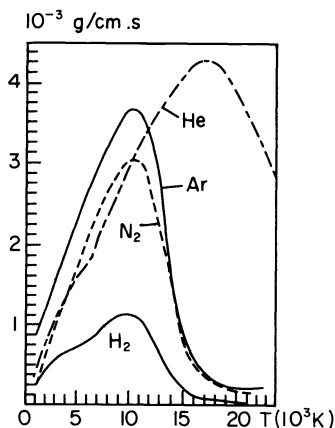


Fig. 28: Evolution of viscosity of He, Ar, H₂, N₂ versus temperature.

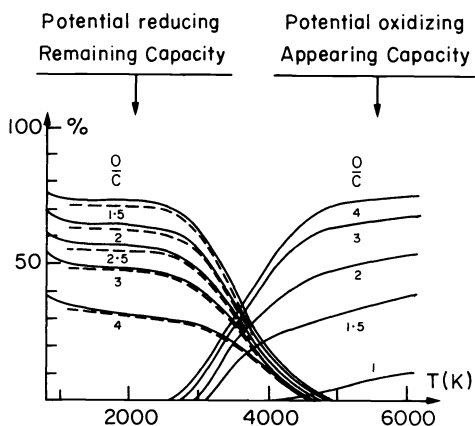


Fig. 29: Evolution of potential reducing and oxidizing capacity of the gas mixture versus the temperature for different ratios O/C at P=1atm, C/H=1/9.

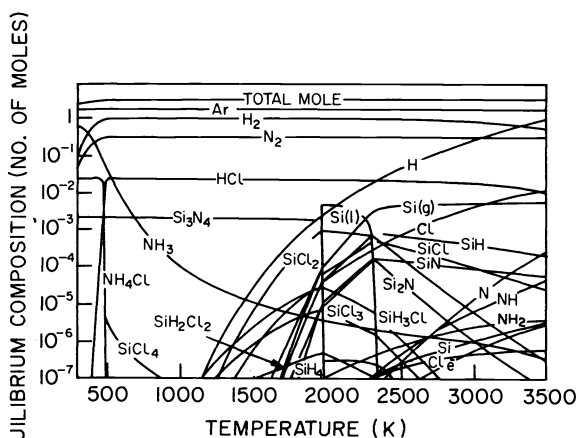


Fig. 30: Thermodynamic equilibrium diagram for the Ar-N-H-Si-Cl system. Ref. (23).

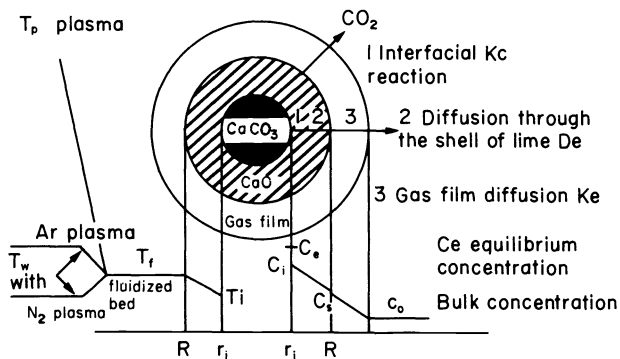


Fig. 32: Limestone decomposition in a fluidized bed plasma reactor.

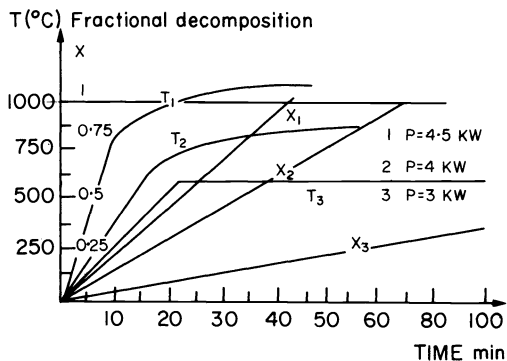


Fig. 33: Fractional decomposition and temperature of CaCO₃ versus time.

For the prediction of the chemical reaction between the material and plasma, complex chemical equilibriums provide the main combinations as function of the thermal data and chemical compositions (figs. 27a to 30) (43). But for the same reasons we are not quite convinced that the chemical composition of the boundary layer is wellknown. Diffusion phenomena, chemical reactions, evaporation, and deposition can modify these predictions and oblige to study by emission spectrometer the mass and heat transfer at the interface.

fig. 31 Comparison of transport properties of an Argon plasma and a liquid silicon

| | Ar | | Si |
|--------------------------------------|--|------------------|-------------------------|
| Viscosity η 10^{-2} g/s.cm | T = 2500 K T = 10.000 K | 0.045 0.3 | 0.3 |
| electrical conductivity mos/cm | T = 5000 K T = 10 000 K | 0.1 0.01 | T = 1400 K 0.1to 100 |
| thermal conductivity W/m.K | T = 2000 K T = 5000 K T = 10.000 K | 0.01 0.1 1 | T = 1400 K 0.0086 |

Calculation of few adimensional number for liquid silicon at 2000 K, for the next experimental condition $\Delta T = 1000^\circ\text{C}$ $V = 0.0166$ cm/s

$$\begin{aligned}
 \text{Re} &= \rho \cdot U \cdot L / \mu &= 14 \\
 \text{Pr} &= \mu \cdot C_p / \lambda &= 0.004 \\
 \text{Gr} &= b \cdot g \cdot \rho \cdot L \cdot \Delta T / \mu &= 7.10 \\
 \text{Sc} &= \mu / \rho \cdot D_c &= 11.85 \text{ for } D_c = 10^{-5} \text{ cm}^2/\text{s} \\
 & &= 118.5 \text{ for } D_c = 10^{-4} \text{ cm}^2/\text{s} \\
 \text{Pe} &= \text{Re} \cdot \text{Sc} &= 165.95 \text{ for } D_c = 10^{-5} \text{ cm}^2/\text{s} \\
 & &= 1659.5 \text{ for } D_c = 10^{-4} \text{ cm}^2/\text{s}
 \end{aligned}$$

IV.2 BOUNDARY LAYERS

Two boundary layers are responsible for the surface treatment: plasma gas boundary and solid or liquid phase boundary. The heat and mass transfer combined with the chemical reactions control the surface treatment.

If the transport properties of the gas and the condensed phase are considered we are surprised by the similitude of some values (fig.31).

However these values are modified by thermal reflectivity, electron diffusion, UV emission, atoms and molecule diffusion. So we cannot talk about barrier zone but of a continuity of the properties between the gas and the surface material.

In that way we propose to compare two cases of surface treatment: treatment with or without phase transition.

IV.3 SURFACE TREATMENT WITHOUT PHASE TRANSITION : ROLE OF THE DIFFUSION PHENOMENA

In order to measure the surface modification during a plasma treatment we have chosen the mechanism of pyrolysis of a limestone powder by its interaction with an argon plasma torch (power=5Kw, P = 1 atm, argon flow feed 23 l/min, average temperature of the gas 5000 K) (fig.32).

In order to analyse a large surface treatment we have chosen to inject the plasma gas inside a fluidized bed of limestone powder ($250 < \phi < 350 \mu\text{m}$) the reaction $\text{CaCO}_3 \rightarrow \text{CaO} + \text{CO}_2 + \Delta H = 167 \text{ KJ}$ has been largely studied and permits to demonstrate that the plasma chemical system is controlled by the external diffusion of mass transfer and/or the external thermal diffusion through the gas boundary layer.

An accordance existing (fig.33) between the modelling of the gas phase diffusion and the experimental data confirms the main role of the boundary layer with a thermal plasma treatment.

The modelling of the kinetic decomposition rate has been realized by Asaki (5) and gives :

$$\frac{dw}{dt} = \frac{4 \pi R_o^2 (C_e - C_o)}{\frac{1}{R T_c K_c (rc)^2} + \frac{R - rc}{D_e M (rc)} + \frac{1}{K_g M}}$$

The integration of this equation over the time reaction leads to the average rate of CaCO_3 decomposition. The fluidized bed temperature and the internal temperature of the particles can be determined by the heat balance on the reactor. In fine the kinetic data of CaCO_3 pyrolysis permit a well comprehension of the exchange through the boundary layer of the particle (fig.34), particularly the heat exchange can be calculated by fitting the model to experimental data versus the reaction temperature of the particles. At last the diffusion phenomena K_g controls the process. These mechanisms can be transposed to surface deposition or evaporation by the plasma phase and permit encapsulation, ceramic protection, or cleaning.

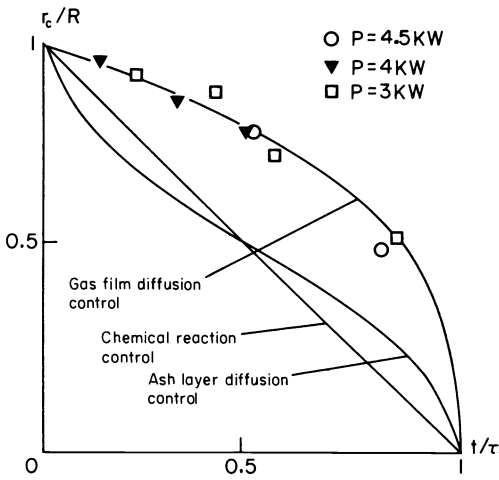


Fig. 34: r/R versus the time for complete reaction.

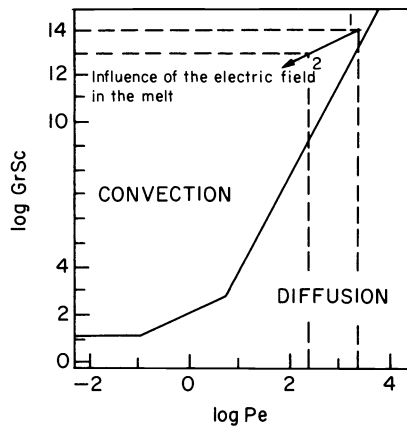


Fig. 35: Domains in the $\log GrSc$ versus the $\log Pe$ plane, corresponding to the different longitudinal macrosegregation regimes. Calculated for: 1: $D=10^{-5}\text{cm}^2/\text{s}$ and 2: $D=10^{-4}\text{cm}^2/\text{s}$.

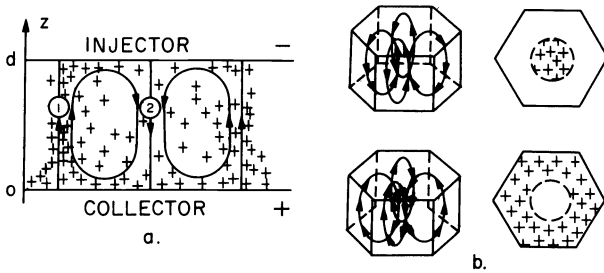


Fig. 36a: Charges injected in the liquid material by the plasma induced convective movement.

Fig. 36b: Orientation of the convective movement as function of the polarization due to the electrical field.

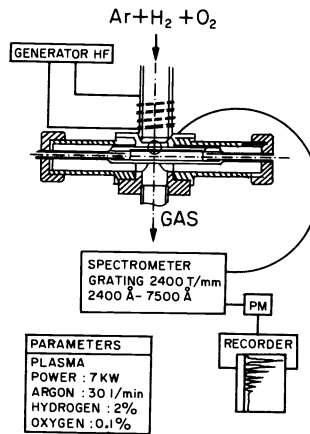


Fig. 37: Experimental apparatus and purification mechanism.

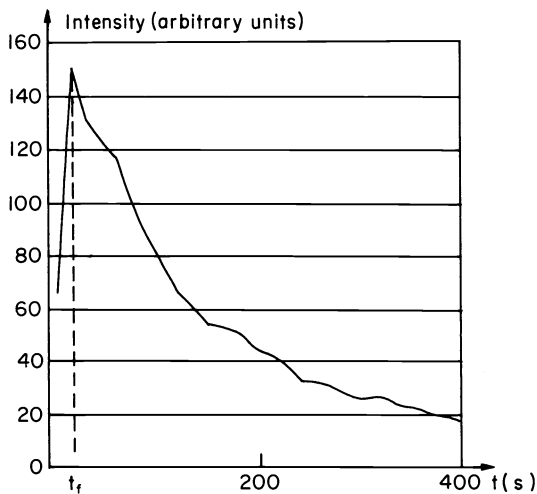
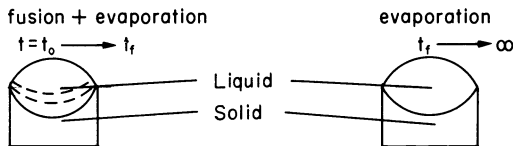


Fig. 38: Static fusion. Atomic emission recording of Mg evaporation. $\lambda=2795.5 \text{ \AA}$.

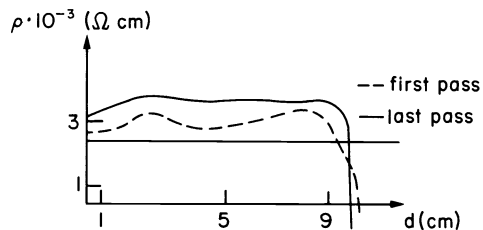
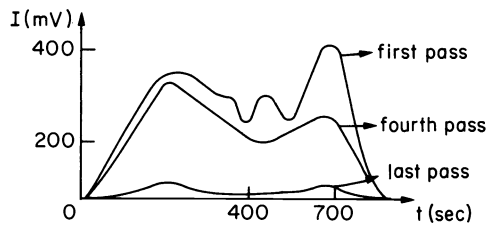


Fig. 39: Correlation between atomic emission signal and resistivity.

IV.4. SURFACE TREATMENT WITH PHASE TRANSITION(spheroidisation, purification, or metal glass production)

By using melting surface treatment and convective phenomenon we increase the degree of freedom of the system and new applications can be developed such as nitriding of liquid steel,(45) spheroidisation of material, refining of metal or silicon,(47,48) and powder of metal glass.(49)

IV.4.1. Heat transfer phenomena between plasma gas and liquid silicon

Taking into account the continuity of transport properties between the plasma and the liquid silicon, the heat transfer at the interface depends on the diffusion, the conduction and the convective phenomena. Nevertheless we can predict the main parameters by calculating the Re , Pr , Gr , Pe and Sc number(50) for the plasma surface melting we observe that convective mechanisms such as Marangoni effect control the heat transfer, so a modelling of heat transfer by using only the conductive phenomena through the interface gas-liquid is generally inaccurate.fig(35)

In addition the electrical field in the plasma induces electrical charges in the material. The induced electrical field in the liquid metal depends on the polarization (anode or cathode) and increases the Marangoni convective phenomena due to the gradient of surface tension by the ionic movement. The electrodynamic movement can rise to 0.1 m/s to 1 m/s during the plasma fusion of the material.(51).fig(36)

V.4.2. Mass transfer phenomena between plasma gas and liquid silicon

Mass transfer through the interface depends firstly on the evaporation rate of the impurities or the raw material(52,53,54) secondly on the chemical reactivity between volatile species, thirdly on the convective movement correlated with the viscosity, the surface tension and the heat transfer(50,55,56).

We have begun an experimental study on the evaporation phenomena during the plasma refining by using the emission spectroscopy at the interface plasma-silicon. To correlate the surface evaporation and the emission spectroscopy we have measured the resistivity of the silicon before and after the plasma treatment.fig(37)

The evaporation phenomena depend on the depth of the liquid zone, in other words on the melting velocity, on the surface of the melting material, and on the temperature of the surface, and at last on the vapor pressure of the element.

In the case of silicon refining, the Magnesium evaporation(fig. 38,39) measured by emission spectroscopy depend at the beginning on the heat transfer phenomena and provides a fusion rate approaching 300 cm/h, while the evaporation phenomena seem to be a first order kinetic rate such as (for the study state fusion) $(1/V)(dNMg/dt)=K(NMg/V)$ with $K= 0.006 s^{-1}$ in our conditions.

By using an oxygen/argon plasma treatment we have pointed out the possibility of boron elimination by slag formation fig.(40). The increase of the number of interface (liquid material, slag, gas) authorized large applications of this technic such as encapsulations, ceramic synthesis, or steel nitriding(57,58,59,60)fig(41)

V-CONCLUSION

For plasma surface treatment it is indispensable to determine the correlation between the plasma properties and the surface evolution of the material. A specific treatment proceeds from a control of the plasma chemical composition according to the needed physical properties.

The large development of the surface treatment by plasma have to take into account constraints of the industrial applications, in that way it seems to be important to characterize the boundary layers between plasma and the material. Some of the properties of the boundary layer can be predicted by thermodynamic calculations others by modelling of the unsteady state phenomena but we can analyze the real heat and mass transfer to be sure that unusual phenomena do not occur, a large part of surface treatment depend on complex chemical equilibrium between the surface and plasma. In the case of non-equilibrium process, these mechanisms depend on electronic excited species i.e on the nature of the electrical power. The large degree of freedom of the reactor surface treatment explain the rapid evolution of the process, plasma polymerization or plasma etching are probably the best examples of the large complex plasma systems which are being explored to solve a lot of constraints such as hazardous gases, etching rates, control process, material evolution, surface pollution etc. A large part of these phenomena which control the quality of the surface treatment can generally be accessible by the emission spectroscopy or laser Raman spectroscopy of the boundary layer.

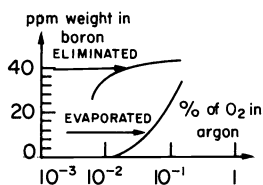


Fig. 40: Elimination of boron by evaporation and drainage as a function of the percent oxygen content in the plasma Raw material: electronic grade silicon 0.011 cm that is 74 ppm by weight of boron. Results obtained after four passes at 40 cm/h.

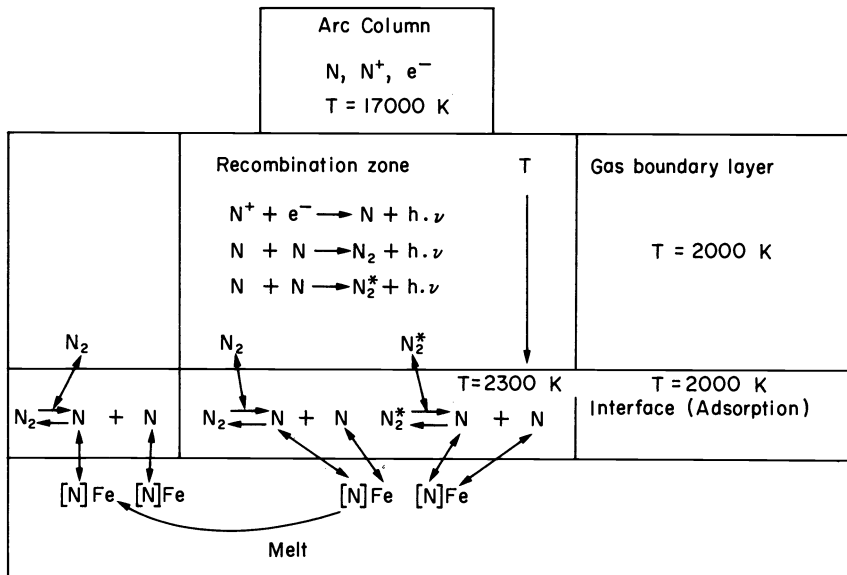


Fig. 41: Schematic representation of mechanism of nitrogen Pick-up in Steel under plasma conditions (Ar/N₂) After (45).

REFERENCES

1. A. Von Engel Ionized gases Clarendon: Oxford (1955).
2. M. Capitelli and E. Molinari Topics and Current Chemistry Vol 90, pp.60 (1980).
3. F. Cramarossa, G. Ferraro, E. Molinari J. Quant. Spectr. Rad. Transf. **14**, 419-436, (1973).
4. J.C. Polanyi J. Chem. Soc. Farad. Trans. , 389-409, (1973).
5. J.C. Polanyi and M.H. Wong, J. Chem. Phys. **51**(4), 1439-1450, (1969).
6. J.H. Mc Creery and G. Wolken, J. Chem. Phys., **66**(6), 2316-2321, (1977).
7. B. Halpern and D.E. Rosner, J. Chem. Soc. Farad. Trans., **60**, 1883-1912, (1977).
8. R. D'Agostino, F. Cramarossa, S. De Benedictis, G. Ferraro, Plasmachemistry and plasma Processing, **1**, 1, 19-35, (1981).
9. D. Rapakoulias, J. Amouroux, M.P. Bergougnan, A. Gicquel, Rev. Phys. Appl., **17**, 95- 101, (1982).
10. M.P. Bergougnan, A. Gicquel, J. Amouroux, Rev. Phys. Appl. **18**, 335-346, (1983).
11. A. Gicquel, M.P. Bergougnan, J. Amouroux, Proceed. of the 4th Symposium on Plasma processing Electrochemical Society, **83**, 10, 169-174, (1983).
12. A. Ricard, Ann. Chim., **8**, 303,312, (1983).
13. A. Goldman and J. Amouroux, Chap. "Plasma Chemistry", 293-345, (1983), Electrical Breakdown and Discharges gases- Part B., Macroscopic processes and discharges. Ed. by E.E Kunhardt, L.H. Luessen, Plenum Publishing Corp.
14. M. Goldman, M. Lecuiler, M. Palierme, 1982 in Proceedings 3rd Int. Symp. on Gaseous dielectrics, Knoxville, Tennessee, Pergamon, New York.
15. G. Lecayon, Y. Bouizem, C. Le Gressus, C. Reynaud, C. Boiziau, C. Jurel, Chem. Phys. Letters, **91**, 6, 506-510, (1982).
16. P.J. Arpino, Actualite Chimique, **4**, 19-28, (1982).

17. R. Walder, J.F. Franklin, Int. Mass Spectrom. Ion Phys., **36**, 85-91, (1980).
18. K.N. Hartman, S.Lias, P. Ausloos, A.M. Rosenstock, S.S. Schroger, C. Schmidt, D. Martinsen, G.W.A. Milne, Compendium of gas phase basicity and proton affinity measurements U.S. N.B.S. Washington DC. (1979).
19. C.R. Moylan, J.I. Brauman, Ann.Rev. Phys. Chem., **34**, 187-215, (1983).
20. M. Berthelot, J.F. Gal, Act. Chimique, **2**, 19-23, (1984).
21. M. Fusio, R.T. Mc Iver, R.W. Taft, J. Amer. Chem. Soc., **103**, 4017-4029, (1981).
22. P. Chang, San Diego, Plasma etching and plasma Technology, 2d Int. Conf. Nov. 1984.
23. H. Yasuda, J. Polymer Sc. Macromol. Rev. **16**, 199-293, (1981).
24. A.T. Bell, Topics in Current Chemistry, **94**, 43-68, (1980).
25. F. Arefi, J. Amouroux, M. Goldman, Advances in low temperature plasma chemistry, Technology applications, Vol. 1, 344-357, (1984).
26. B. Ranby and J.F. Rabek Singulet oxygen, Reactions with organic compounds and Polymers, Wiley- Interscience. Chichester (1978).
27. L. Gillepsie, The electronic repulsion theory of chemical bond, W.L. Luder ed., Dunod, Paris, (1967).
28. J. Amouroux, M. Goldman, F. Arefi, F. Rouzbehi, French Patent No 83125 (1983), U.S. Patent No 634.741 (1984), Japon Patent No 158533 (1984), Eur. Patent 401592.5/1984.
29. F. Arefi, Doctorat Ing. Docteur Thesis, Universite P. et M. Curie, (1984).
30. E. Kry, L.L. Levenson, W.J. James, K.A. Averbach., J. Phys. Chem., **84**, 1635-1638, (1980)
31. O. Demuth, r.Cuelho, J. Amouroux, M. Goldman, IEEE proceedings, Toulouse, 1983.
32. R.K.Sadhir, W.J. James, R.A. Averbach, Thin Solar Films, 17-29, (1982).
33. D.R. Secrist, J.D. Mackenzie, Bul. Am. Ceram. Soc., **45**, 784-770, (1966).
34. N. Inagaki, T. Nischio, K. Katsunta, J. of Polym. Sci. Lett. Ed, **18**, 765-770, (1980).
35. A.R. Reinberg, Ann. Rev. Mater. Sci., **9**, 341-373, (1979).
36. B.R. Loy, J. of Polym. Sci. Part A, **1**, 2251-2259, (1979).
37. L.J. Forrestal, W.G. Hodson, J. of Polym. Sci., **2**, 1275-1280, (1984).
38. H. Fischer, K.H. Hellwege, J. of Polym. Sci., **56**, 33-45, (1962).
39. C. Sar, M. Valentin, Bui Ai, J. of Appl. Polym. Sci., **24**, 503-516, (1979).
40. M. Capitelli, E. Ficocelli, E. Molinari, Equilibrium compositions and Thermodynamics properties of mixed plasmas. University of Bari, (1970).
41. P. Fauchais, J. Aubreton, Rev. Phys. Appl., **18**, 51-66, (1983).
42. J. Amouroux, J.L. Codron, D. Morvan, Ann. Chim. Fr, **3**, 59-78, (1978).
43. T. Yoshida, H. Endo, K. Saito, K. Akashi, ISPC-6, Montreal, A-7-3, 1,225-230, (1983).
44. Y. Asaki, Y. Fukunara, T. Nacasse and Y. Kondo, Metallurg. Trans. **5**, 381-390, (1974).
45. T.E.L. Gammal, G. Hinds, W.Hascing, J. Vetter, Proc. 7th ICVM. Tokyo, **21.2**, 1044-1051, (1982).
46. N.N Rykalin, Pure and Appl. Chem. **52**, 1801-1815, (1980).
47. D. Morvan, J. Amouroux, Plasma Chemistry and Plasma Processing, **1,4**, 397-418, (1981).
48. D. Morvan J. Amouroux, M.C. Charpin, H. Lauvray, Rev. phys. Appl. **18**, 239-251, (1983).
50. D. Camel and J.J Favier, J. of Crystal Growth, **67**, 42-67, (1984).
51. B.E Paton, B.I Medovar, Yu. G. Emelianenko, S. Yu. Andrienko, Ev. Scherbinin, A.I. Chaikovskii, A. Yu. Chudnovskii, Proc. 7th ICVM, 1982, 1527-1533, Tokyo.
52. Y. Chen, E. Pfender, Plasma Chemistry and Plasma processing, **3**, 97-112, (1983).
53. J.M. Badie, P. Chaussade, C.Bonet, ISPC-6. Montreal, A-6-7, **1**, 205-210, (1983).
54. D. Cubicciotti Pure and Appl. Chem. **57**, 1-13, (1985).
55. A. Lacour, A. Accary, ISCP-6, Montreal 1983, A-1-5.
56. A.V. Bolotov, V.N Musolin, A.V. Kolesnikov, H.N. Philkov, ISPC-6, Montreal, A-7-5, **1**, 237-241, (1983).
57. Yu. Latash, G.F. Torkhov, V.K.Granovsky, Proc. 7th ICVM. Tokyo, **2**, 1052-1059, (1982).
58. C.B. Alcock. Pure and Appl. Chem. **52**, 1817-1827, (1980).
59. P. Fauchais, Rev. Phys. Appl., **15**, 128-130, (1980).
60. G.R Kubanek, W.H Gauvin, G.A. Irons, H.K. Choi, ISPC-4, Zurich, 27-31, (1979).
61. E. Pfender, Electric Arcs and Arc Gas Heaters, in Gaseous Electronics, Vol.1, Electrical Discharges, Ed. Merle N. Hirsch, H.J. Oskam, Academic Press, New York, (1978).